Experimental characterization of Italian composite adobe bricks reinforced with straw fibers

Fulvio Parisi [a,1], Domenico Asprone [a], Luigi Fenu [b], Andrea Prota [a]

[a] *Department of Structures for Engineering and Architecture, University of Naples Federico II, via Claudio 21, 80125 Naples, Italy*

[b] *Department of Civil Engineering, Environment Engineering, and Architecture, University of Cagliari, Piazza d'Armi, 09123 Cagliari, Italy*

Abstract

Adobe buildings are located in many countries and are often constructed with fiber reinforced bricks, which are composite materials made of soil, water, and natural or artificial fibers. This study presents experimental findings for straw fiber reinforced adobe bricks typically used in Sardinia (Italy) and produced according to traditional worldwide handcrafted manufacturing procedures. A large number of compression and three-point bending tests were carried out on cubic and prismatic specimens, respectively. The identification of significant scatter in experimental data sets due to handcrafted manufacturing motivated the estimation of mechanical parameters at different percentile levels, in order to provide their characteristic and median values. The geometry of straw fibers was statistically characterized in terms of mean, standard deviation and probability distribution of their diameter and length. The mechanical characterization in compression included the estimation of fracture energy. Bending test data were processed to estimate Young's modulus in tension, highlighting the bimodularity of the earthen composite material. Finally, both elastic–perfectly plastic and nonlinear stress–strain models are proposed for design/assessment purposes.

Keywords

Adobe bricks; Straw fibers; Experimental tests; Mechanical behavior; Stress–strain models

DOI: https://doi.org/10.1016/j.compstruct.2014.11.060
Article published in: Composite Structures
Volume 122, April 2015, Pages 300-307

[1] Corresponding author. Tel.: +39-081-7683659; fax: +39-081-7685921.
E-mail address: fulvio.parisi@unina.it (F. Parisi).

1. Introduction

Earthen construction has been one of the most largely used construction techniques in different historic ages. Man began to use earthen construction at least 5000 years ago [1], [2] in Mesopotamia and Turkmenistan and it has been largely used by different civilizations all around the world. Nowadays it is estimated that between 30% and 50% of world population lives in earthen structures [3], mainly in some regions of Africa, Asia and Latin America, where earthen construction techniques are still largely used for new dwellings. Even in Europe, new earthen structures are built as a niche product of construction industry, mainly to ensure comfort to occupants and architectural compatibility with historical built environments. In fact, 10% of the UNESCO World Heritage properties includes earthen structures. Also in Europe the historic centers of Cordoba, Oporto, Lyon, Guimarães are some of the UNESCO sites where earthen structures are largely present [4].

Therefore, material scientists and civil engineers are largely interested in earthen construction and many scholars are working on this topic. The interest in this kind of structures is motivated not only by the large spread all over the world, but also by their poor mechanical properties resulting in high structural vulnerability against natural hazards (e.g. earthquakes, floods). Even though many scientific works on different types of earthen materials and structures are available in literature [5], [6], [7], [8], [9], detailed studies are needed to assess material properties and structural behavior because earthen structures are strongly site-specific, depending on the techniques used for material production and on-site construction of the building. This research effort is rapidly increasing also in Italy, where several examples of earthen buildings are still present, especially in Piemonte, Marche, Abruzzo, Emilia Romagna and Sardinia [10], [11]. The latter is the second biggest island (besides Sicily) in the Mediterranean Sea and the Italian region with the highest number of earthen buildings. Until the beginning of the Second World War, almost all the buildings in the villages of the alluvial plain of Campidano (Sardinia) were typically built with earth, that was the only construction material available there. Indeed, that alluvial plain was the part of Sardinia with more fertile soil and richer agriculture production. It was estimated that those villages had more than 10,000 inhabitants living in about 30,000 earthen buildings until the 50's of the past century. In the second half of 1900, about half of those buildings were demolished, but in the last fifteen years there has been a revival of earthen architecture so that new earthen buildings have been constructed. The most used earth construction technique in Italy is the *adobe masonry*, which is an assemblage of adobe bricks and mud mortar. On the other hand, *pisé* or *rammed earth* is produced by ramming and compacting earth in a formwork and, in Italy, is mainly used in Piemonte. Adobe bricks are made of a dry mixture of soil, water and straw [12] and are usually obtained by pressing the soil mixture into a prismatic formwork and then drying each brick through the combined action of air and sunshine. In some countries, several additives are also added to the soil mixture. In the case of Sardinia, the mixture of adobe bricks was typically stabilized with dung and urine in the past. Nowadays, cement is sometimes added to the mix of modern Sardinian adobe bricks in order to increase strength and reduce erodibility, as it also happens by adding lime.

In this paper, traditional adobe bricks manufactured in Solarussa (a small village in the middle west of Sardinia) are physically and mechanically characterized by laboratory testing. Those bricks are produced as a mixture of soil, water and straw fibers, and are usually sold for construction of new earthen buildings or restoration of old ones. It is recognized the fundamental role of fibers in reducing shrinkage cracking in adobe bricks, thus improving the behavior of adobe masonry. This study is the first step of a larger research program [13], [14], [15] aimed at assessing and reducing the seismic vulnerability of adobe buildings in Sardinia, after its inclusion in the seismic zone model of the Italian territory. In this respect, it is emphasized that existing adobe buildings in Sardinia were not designed for earthquake resistance, revealing a pressing need for their assessment and retrofit. Therefore, this research program falls within a strategic plan of the Sardinian Regional Administration for earthquake protection of people and property.

2. Experimental program and results

The straw fiber reinforced adobe bricks under study were 100 × 200 × 400 mm^3 in size and had a mean unit weight equal to 16.80 kN/m^3 with coefficient of variation (*CoV*) equal to 2%. Every brick had a grooved surface to get satisfactory brick–mortar bond in adobe masonry (Fig. 1). Adobe bricks were produced by one of the three traditional manufacturers that still work in Sardinia, Italy, hence providing a clear impact of this study on knowledge and use of this building material.

Fig. 1. Straw fiber reinforced adobe brick.

The manufacturing process of adobe bricks was almost completely based on manufacturer's experience, only requiring an electrical mixing machine and a mechanical straw chopper that randomly cut straw fibers with length lower than 100 mm. According to the traditional brick manufacturing of adobe bricks in Sardinia, Italy, the composition of the mixture was provided by volume using a pail and the water content of straw fibers was not controlled. After a first mixing stage including addition of randomly oriented straw fibers, some water or soil was typically added to the mixture in the mixing machine, depending on the mixture appearance evaluated by the manufacturer. Then, prismatic wood formworks with internal size equal to that of bricks were filled with the mixture, which was pressed by hand but without measuring the degree of compaction. In the last stage of manufacturing process, the adobe bricks were dried under the sun to ensure water removal. As adobe bricks were manufactured through a handcrafted process, they may be considered as a nonengineered building material to characterize from a mechanical viewpoint in order to assess structural performance of adobe buildings in Sardinia. It is stressed that the Sardinian manufacturing process is similar to traditional procedures used in less developed countries in Asia and Africa.

The experimental program carried out by the authors consisted of: (1) a physical characterization including particle size distribution analysis of the soil of the adobe bricks and statistical analysis of the length of straw fibers added to the soil mixture; (2) uniaxial compression tests on cubic specimens; and (3) indirect tensile tests based on the three-point loading scheme for prismatic specimens. The straw fiber length was statistically analyzed because fibers were randomly cut and added to the soil–water mixture. Cubic and prismatic specimens were taken out from adobe bricks. Laboratory technicians paid particular attention when cutting bricks, in order to avoid any modification in specimens' consistency. Specimens were prepared in laboratory under controlled temperature and relative humidity.

2.1. Physical characterization

Physical characterization tests provided the density, water content, grain size distribution of the soil used for the fabrication of adobe bricks, and also geometrical properties of straw fibers. Density and water content of the soil used for brick fabrication were found to be 2.68 g/cm^3 and 27%,

respectively. The particle size distribution was obtained by sieving (for particle size greater than 75 μm) and hydrometer analysis (for the soil fraction passing through a 200 mesh sieve, i.e. 75 μm). Atterberg limits (i.e. liquid limit, plastic limit, and plasticity index) cannot be measured owing to the high percentage of sand, as shown by the grain size distribution of the soil (Fig. 2). Sieve analysis was carried out according to ASTM D2487-11 standard [16]. The lack of values for Atterberg limits did not allow the distinction between silt and clay fractions, so that sieve analysis provided the following percentages by weight: 26.9% of clay and silt (grain diameter $d_g < 0.075$ mm), 70.1% of sand (0.075 mm $< d_g <$ 4.75 mm), 3% of gravel (4.75 mm $< d_g <$ 75 mm). Therefore, the soil was classified as clayey/silty sand, which belongs to the class of coarse-grained soils with fines [16]. The particle size distribution of the soil in Fig. 2 indicates that the soil is suitable for earth construction, according to local traditional practice in Sardinia, Italy. Indeed, the following ranges are typically used in that region [17]: 22–53% of clay and silt; and 55–75% of sand and gravel.

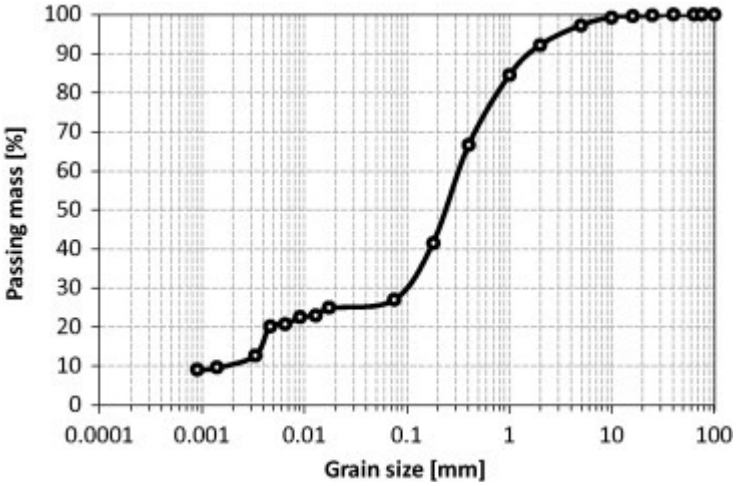

Fig. 2. Grain size distribution of adobe bricks.

Straw fibers were added to the soil–water mixture ensuring a random distribution of straw fiber reinforcement within the brick volume and stabilization of adobe bricks (i.e. lack of shrinkage cracking). The distribution of straw fiber length within adobe bricks was also characterized. To that end, three bricks were entirely submerged and dissolved in water for about four days. Straw fibers were completely separated from the soil without specific mechanical devices, but further research is needed to characterize the bond between straw fibers and soil. That procedure allowed the authors to obtain three samples of straw fiber reinforcement (Fig. 3), finding that fibers had mean diameter of 3 mm ($CoV = 7\%$), mean length of 70 mm ($CoV = 34\%$), and mean percentage by weight of 0.64% ($CoV = 21\%$). Fig. 4 shows the histogram of straw fiber length and the fitted lognormal probability density function (PDF), which could be used in probabilistic modeling of adobe bricks. It is noted that fiber fraction by weight is typically between 0.5% and 3% in Sardinia, whereas fibers are not longer than minimum dimension of bricks, which is generally 100 mm [17], [18]. Finally, it is also emphasized that the geometry of straw fiber reinforcement was characterized to provide information for micromechanical studies aimed at deriving the mechanical behavior of adobe bricks on the basis of its actual composition at the microscale (i.e. grains, voids with and without water, and straw fibers).

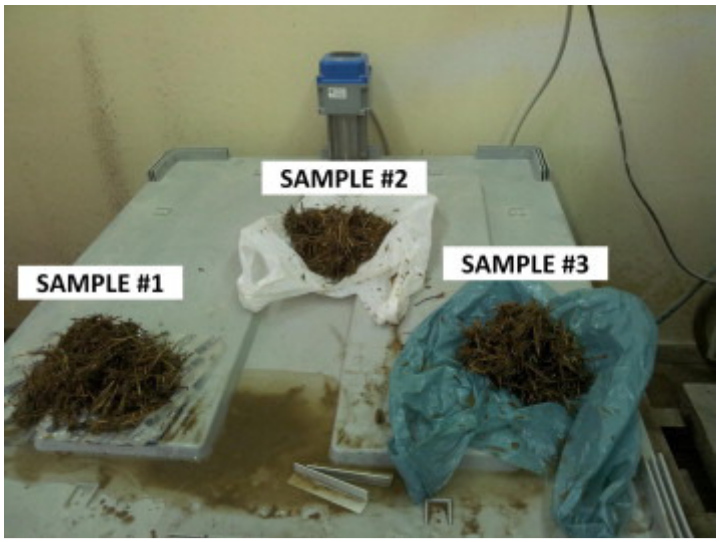

Fig. 3. Straw fiber samples from individual adobe bricks.

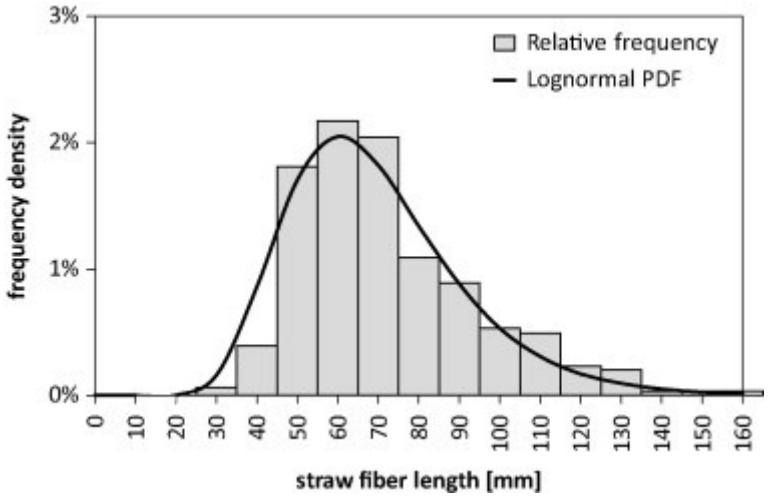

Fig. 4. Histogram of straw fiber length and fitted lognormal PDF.

2.2. Mechanical characterization

2.2.1. Uniaxial compression tests

The mechanical behavior of adobe bricks in compression was characterized through displacement-controlled uniaxial tests, according to European standards [19]. Specimens were cubes with 70 mm edge and were placed between rigid steel plates of the MTS810 universal testing machine. The loading procedure consisted of two initial cycles, which were followed by displacement-controlled monotonic loading at a displacement rate of 0.01 mm/s. Load measurements were directly provided by the testing machine in real time. Axial displacements of cubic specimens were measured by both the testing machine and four linear variable differential transducers (LVDTs), which were fixed on the four sides of the rigid end plates of the machine. It is however underlined that stroke and LVDT readings provided the same average displacements of specimens. Conversely, it was not possible to get direct measurements of axial strains because of poor bond between strain gauges and adobe specimens.

Sampling frequency was set to 1 Hz in the data acquisition system. The initial loading cycles were aimed at providing adequate contact between specimen and rigid plates; they consisted in the

application of a compressive force ranging between 0.5 kN and 1 kN, in order to get an elastic response of specimens. Each test was stopped when compressive load reached one-fourth of its maximum value in the post-peak descending branch of the load–displacement curve. This allowed the authors to quantify most part of strain ductility and fracture energy of cubes.
Uniaxial compression tests were carried out on 34 cubic specimens deriving the stress–strain curves in Fig. 5, which reveals significant scatter in compressive behavior. The following mechanical properties are outlined in Table 1: peak compressive strength f_c; axial strain at peak compressive strength ε_p; secant Young's modulus at one-third of peak strength $E_{1/3}$; secant Young's modulus at one-half of peak strength $E_{1/2}$; and compressive fracture energy G_{fc}. For each of the aforementioned properties, the characteristic value $x_{0.05}$ (that is, the value which is not exceeded by 5% of specimens) was estimated in addition to sample mean μ and CoV. Table 1 demonstrates that CoV is between 29% and 40%. The modulus of elasticity $E_{1/2}$ was estimated in accordance to American standards [20] and was the most dispersed mechanical property (CoV = 40%). Mean compressive strength and secant Young's modulus were similar to those estimated in the case of Portuguese adobe bricks extracted from land dividing walls [21].

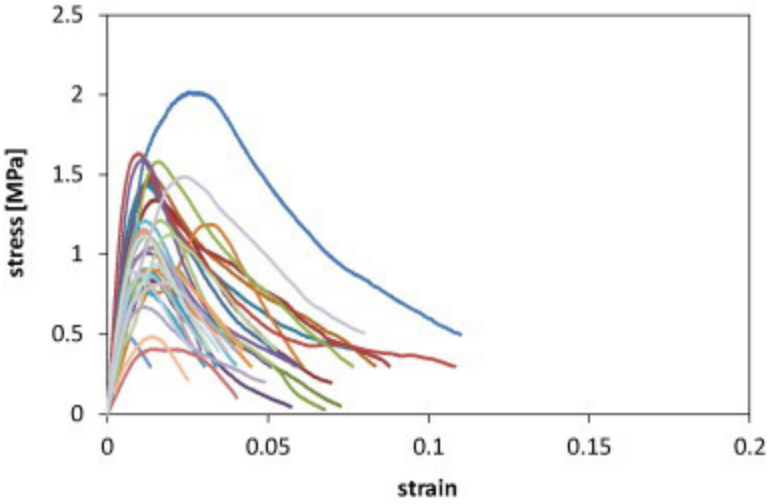

Fig. 5. Experimental stress–strain curves for adobe bricks in compression.

Table 1. Mechanical properties of adobe bricks in compression.

Value	f_c **(MPa)**	ε_p **(%)**	$E_{1/3}$ **(MPa)**	$E_{1/2}$ **(MPa)**	G_{fc} **(N/mm)**
$x_{0.05}$	0.46	0.79	69	54	1.87
μ	1.08	1.35	145	143	3.36
CoV	36%	29%	37%	40%	33%

Based on compression test results, the authors performed a robust regression analysis which provided the linear correlation $E_c = 129 f_c$ (with coefficient of determination $R^2 = 0.83$) between the secant Young's modulus E_c (assumed to be the elastic modulus $E_{1/3}$) and peak compressive strength. Details on that analysis and plots can be found in [15]. It is noted that recent tests on Portuguese

adobe bricks from houses and land dividing walls provided $E_c = 173f_c$ [21], whereas the New Zealand standard NZS 4297:1998 [22] recommends to assume $E_c = 300f_c$.
Compressive fracture energy was directly computed as the integral of the post-peak descending branch of the stress–displacement diagram, according to standard definitions for quasi-brittle materials (see for instance [23]). The mean value of G_{fc} was found to be 3.36 N/mm, but the characteristic value (which was equal to 1.87 N/mm) could be a more conservative assumption. The following nonlinear correlation between compressive fracture energy and peak compressive strength was found ($R^2 = 0.45$):

Gfc=4.12fc-4.02fc2 (1)

as depicted in Fig. 6 (see the dashed line). In most cases, a linear correlation model allows to reduce computational work so it was fitted to experimental data, providing $G_{fc} = 3f_c$ with $R^2 = 0.35$ (solid line). It is noted that such correlations provide compressive fracture energy in N/mm if compressive strength is expressed in MPa.

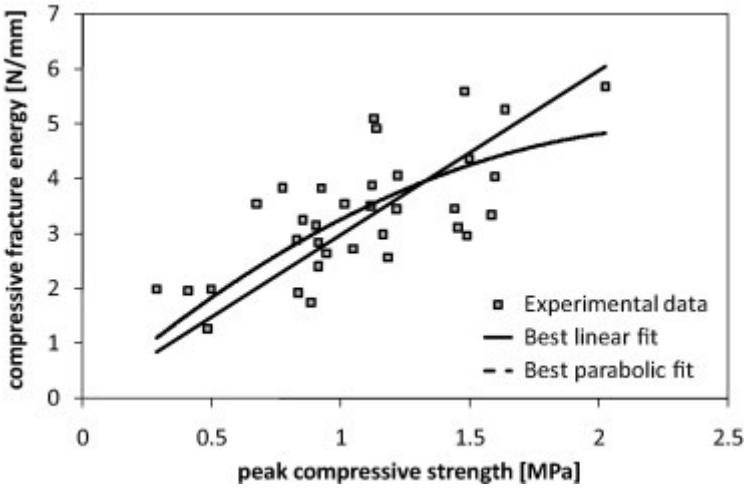

Fig. 6. Compressive fracture energy versus peak compressive strength.

Finally, the elastic–perfectly plastic (EPP) model was assessed because it is often used to simulate compressive behavior of masonry units and also entire masonry assemblages in simplified structural models [24], [25]. To this end, the elastic range was assumed to be linear with Young's modulus E equal to the secant experimental modulus at a stress level of $0.7f_c$. The ultimate strain ε_u was assumed to be the experimental strain at a stress level of $0.8f_c$ (i.e., 20% strength drop) on the post-peak softening branch. Ultimate compressive strength f_{cu} and the corresponding cracking strain ε_e were thus derived by assuming equal areas below the experimental and idealized stress–strain diagrams. Therefore, an available strain ductility factor in compression $\mu_\varepsilon = \varepsilon_u/\varepsilon_e$ was evaluated for adobe bricks in order to quantify their fracture energy in a simplified way. Fig. 7(a) shows the bilinear idealization of a typical experimental stress–strain curve, whereas idealized EPP diagrams of all specimens are plotted in Fig. 7(b). It is emphasized that: (1) strain ductility is just a fictitious parameter that is used to define an upper bound to inelastic strains for quasi brittle materials; and (2) by definition, ultimate strength cannot exceed the actual compressive strength of bricks. Table 2 provides statistics for the idealized stress–strain diagrams. Mean values of cracking

and ultimate strains are significantly larger than those typically assumed for concrete and clay brick masonry as a whole, which are 0.2% and 0.35% respectively.
The EPP model introduced here for adobe bricks can be used for design purposes, while nonlinear constitutive models are recommended for assessment purposes.

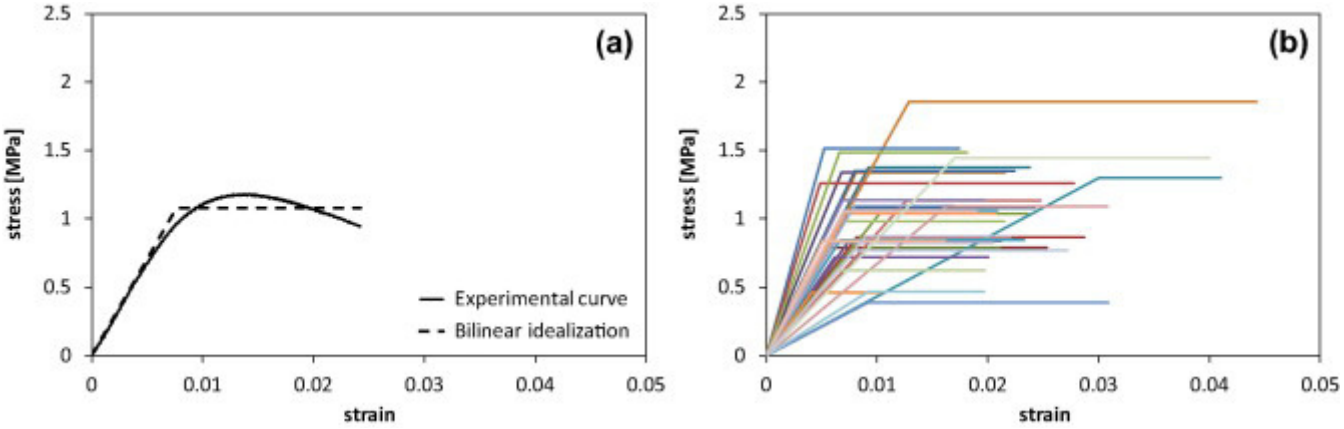

Fig. 7. (a) Bilinear idealization of typical stress–strain curve and (b) idealized stress–strain diagrams.

Table 2. Properties of idealized EPP stress–strain diagrams in compression.

Value	f_{cu} **(MPa)**	E **(MPa)**	ε_e **(%)**	ε_u **(%)**	μ_ε
$x_{0.05}$	0.47	48	0.50	1.66	3.30
μ	1.03	132	0.88	2.37	2.70
CoV	32%	41%	54%	30%	26%

2.2.2. Three-point bending tests

Mechanical behavior of straw reinforced adobe bricks in tension was investigated by means of three-point bending tests, which belong to the class of indirect tensile tests together with splitting tests. By the way, it is observed that existing standards and recommendations on earthen construction materials (see, e.g. [22], [26], [27], [28], [29]) do not specify size and geometry requirements for specimens to be tested in flexure. Therefore, three-point bending tests were carried out on 36 prismatic specimens according to the European standard EN 1015-11 [30]. The specimens were extracted from adobe bricks and were 40 × 40 × 160 mm^3 in size, in order to avoid arching effects in the flexural resisting mechanism. Each specimen was placed over steel supports in a way to obtain a clear span length of 100 mm, whereas a concentrated load was applied at the mid-span section. All tests were performed through the universal machine used for compression tests. Load–deflection curves were derived through displacement-controlled monotonic loading at a displacement rate of 0.01 mm/s. The applied load was measured by the load cell of the testing machine, whereas the deflection at the mid-span section was measured by the testing machine (as stroke readings) and one LVDT at the bottom, providing about the same measurements. Loads and displacements were recorded by the data acquisition system at a sampling frequency of 1 Hz. Load–deflection records were corrected by removing the first branch with apparent stiffness increase, in order to eliminate the initial contact effect between specimen and test setup. As a result, corrected load–deflection curves were shifted back to the origin of coordinate system, removing initial deflection due to contact. Experimental load–deflection curves of all specimens are depicted in Fig.

8(a). The elastic behavior was essentially linear up to the peak load, which was followed by a sudden load drop with very limited fracture energy.
According to EN 1015-11 [30], tensile stresses can be computed by means of Euler–Bernoulli beam theory of uniaxial bending as follows:

$$f_t=1.5Fl/bd^2 \qquad (2)$$

where F is the applied load; l is the span length; b and d are respectively the width and depth of the mid-span section.

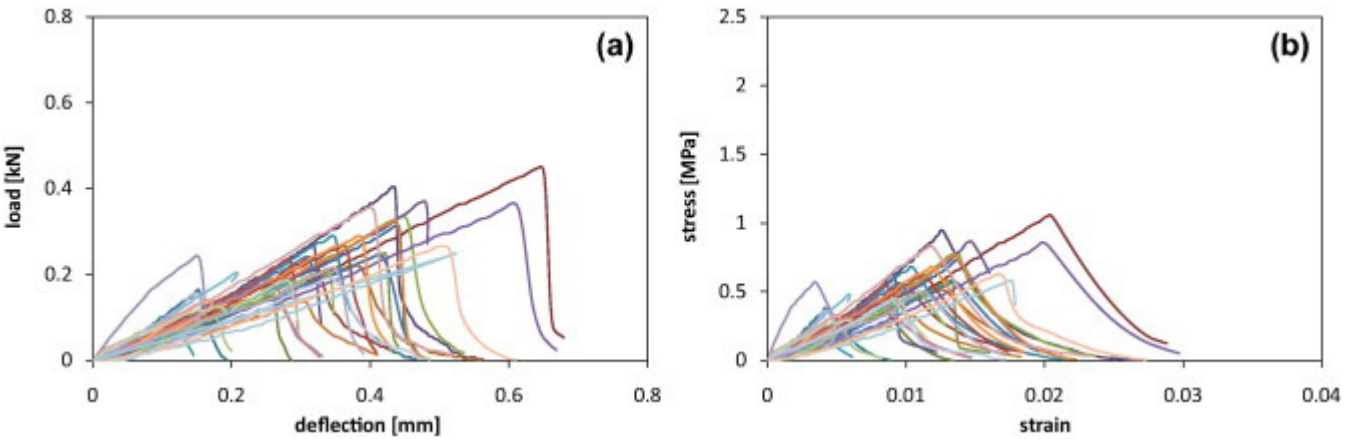

Fig. 8. (a) Experimental load–deflection curves and (b) experimental stress–strain curves in tension corresponding to mean secant Young's modulus in compression

In such a case, the adopted standard [30] allows one to neglect the arching action that occurs in the blocks as a result of small span to depth ratios. Nevertheless, no standard rules are presently available for transformation of deflections to tensile strains at the bottom edge of prismatic specimens. In line of principle, it can be assumed that the straw fiber reinforced earth material under study is a bimodulus material, namely, it has different elastic moduli in tension and compression. This is a realistic assumption because most materials (including concrete, ceramics, graphite, and some composites) experience different strains in tension and compression under the same (absolute) level of tensile and compressive stress [31], [32]. Effects of this assumption on mechanical behavior of adobe masonry were assessed by micromechanical analysis in [13], [14]. Material bimodularity causes different stress–strain relations for the fractions of cross section above and below neutral axis under uniaxial bending. As a result, in the elastic range one can apply the homogenization approach of elastic beam theory. If the mid-span section of a single prismatic adobe specimen is considered and the ratio of the tensile Young's modulus to the compressive Young's modulus is denoted as $n = E_t/E_c$, balance equations of the beam cross section provide the neutral axis depth x_n and the ratio n as follows:

$$x_n=(3I_n/bd)^{1/2} \qquad (3)$$

$$n=3In / [bd3-2(3bd3I_n)^{1/2}+3I_n] \qquad (4)$$

where I_n is the second moment of inertia of the homogenized cross section. Given that the deflection at mid-span section of prismatic specimens was known, it was possible to estimate I_n at each deflection level v imposed during the test as follows:

$I_n = Fl^3/(48E_cv)$ (5)

Therefore, Eq. (4) was used to compute n (and hence Young's modulus in tension) at each deflection level, whereas Eq. (3) was employed to compute x_n, and hence tensile stress and strain at the bottom of specimen. Eq. (5) leads to establish a dependence of the estimated tensile Young's modulus on the assumed compressive Young's modulus. Given that Young's modulus of adobe bricks in compression was found to be scattered, such a procedure was used to compute stress–strain curves in tension corresponding to three values of E_c: $\mu - \sigma = 91$ MPa; $\mu = 145$ MPa; and $\mu + \sigma = 198$ MPa. Herein, σ stands for standard deviation of any random variable. Fig. 8(b) shows experimental stress–strain curves in tension corresponding to mean secant Young's modulus in compression (i.e., $E_{cm} = 145$ MPa). Estimates of Young's modulus in tension are given in Table 3 accounting for variability over the 36 specimens considered in this study.
Characteristic tensile strength was found to be 0.28 MPa, while mean tensile strength and standard deviation were respectively equal to 0.56 MPa and 0.20 MPa (corresponding to $CoV = 36\%$). The mean of n was then equal to 0.4 with $\sigma = 0.17$ (i.e., $CoV = 43\%$) when the mean secant Young's modulus in compression was assumed. Such an outcome demonstrates that the straw fiber reinforced earth material under study can be assumed to be a bimodulus material, namely the assumption of different Young's moduli in tension and compression is confirmed. As the procedure discussed above applies to the elastic range and no instruments were used to measure crack width at the mid-span of specimens, fracture energy estimation in tension was not possible.

Table 3. Mechanical properties of adobe bricks in tension.

Value	f_t **(MPa)**	E_c **(MPa)**	E_t **(MPa)**		
			$\mu-\sigma$	μ	$\mu+\sigma$
$\mu - \sigma$	0.36	91	35	69	103
μ	0.56	145	34	58	82
$\mu + \sigma$	0.76	198	33	53	73

3. Comparison with existing experimental data

Table 4 includes the main experimental data available in literature [8], [9], [10], [21], [33], [34], [35], [36], [37], [38], [39], [40], [41], [42], [43], [44], [45] on both strengths and elastic moduli of adobe bricks with and without fiber reinforcement. Those data include fiber reinforcement percentage ranging between 0.25% and 10% of brick weight. The authors collected experimental data related to monotonic behavior of adobe bricks for comparative purposes. Nevertheless, it is noted that few cyclic tests have been carried out and published in literature so far.
In the case of Italian adobe bricks compressive strength, tensile strength, and secant Young's modulus in compression fall in the ranges [0.2 MPa, 2.5 MPa], [0.17 MPa, 0.75 MPa] and [15 MPa, 287 MPa], respectively. The straw fiber reinforced adobe bricks investigated by the authors in this study also fall in such ranges.
If experimental ranges provided by Bouhicha et al. [8] and Galán-Marín et al. [37] are considered, different trends are derived on the variation of compressive strength with fiber reinforcement content. In fact, Bouhicha et al. found that f_c reduced as fiber fraction was increased from 0 to 3.5% in adobe bricks typically used in Algeria, whereas the opposite trend was found by Galán-Marín et al. by testing adobe bricks usually employed in Scotland under varying fiber fraction from 0% to 0.5%. In both experimental studies, the addition of fibers to adobe specimens induced an increase in

tensile strength. In the case under study by Bouhicha et al. and Galán-Marín et al., tensile strength of adobe bricks was found to be approximately half of compressive strength.
The bimodularity of the adobe material, that is, the difference between elastic moduli in tension and compression, was also found by Silveira et al. [43] by testing adobe bricks taken out from typical houses and land dividing walls located in Portugal. Compression tests performed by Meli [41] on unreinforced adobe specimens evidenced a mean compressive strength approximately equal to that derived by the authors, while three-point bending tests led to derive a tensile strength 44% lower than that presented in this study. Mean compressive strength provided by Meli for adobe bricks typically used in Mexico was confirmed by Figueiredo et al. [36]. Very low estimates of compressive Young's modulus were obtained by Fratini et al. [10] and Wu et al. [44].

Table 4. Experimental data on strengths and elastic moduli of adobe bricks.[a]

Source	Location	Fibers (%)	f_c (MPa)	f_t (MPa)	E_c (MPa)	E_t (MPa)
[8]	Algeria	0	4.1–5.1	1.1–2.5		
		1.0	3.6–5.4			
		1.5	3.2–5.6	1.2–2.6		
		2.0	3.0–4.1			
		2.5	2.4–3.7	1.6–2.7		
		3.0	2.3–3.0			
		3.5	2.3–2.7	1.8–2.9		
[9]	Turkey	NA	2.0 (old)			
			2.4–5.1 (new)			
[10]	Italy	0	0.2–0.78 (old)		15–87	
			0.72–2.44 (new)		90–287	
[21][b]	Portugal	0	0.66–2.15	0.13–0.19[c]	51–448	100–340
[33]	Italy	10	2.5			
[34]	Turkmenistan	0	0.94	0.29	193	
				0.20[c]		

Source	Location	Fibers (%)	f_c (MPa)	f_t (MPa)	E_c (MPa)	E_t (MPa)
[35]	Morocco	0	2.83[d]	0.18–0.35		
[36]	Portugal	0	0.46	0.15		
[37]	Scotland	0	2.23–3.77	1.06–1.12		
		0.25	3.05–4.44	1.10–1.45		
		0.5	4.37	1.05		
[38]	Mexico	0	1.18	0.27		
[39]	Italy	0.5	1.57–1.70	0.75	130–148	
[40]	Italy	0	0.29–1.56	0.17–0.40		
[41]	Mexico	0	0.51–1.57	0.20–0.43		
[42]	Colombia	0	3.04	0.41		
[43][e]	Portugal	0	0.28–1.21	0.20–1.03	7609–25,000	
				0.03–0.28[c]		
[44]	China	0.5	1.39–1.70		24.04–41.70	
[45]	Germany	0	2.10–3.75	0.38–0.75[f]		
		0.6		0.15–0.27[f]		
		0.7–3.8	0.55–1.75			
This study	Italy	0.6	1.08	0.56	145	58

a

Single data indicate sample mean; fiber fraction is given as percentage by weight; NA = not available.

b

Aggregated data of specimens taken out from houses and land dividing walls.

c

Data from splitting tests.

d

Data from sclerometer tests.

e

The composition of adobe specimens included a air-lime mortar fraction of 25–40%.

f

Data from direct tensile tests.

4. Proposed constitutive equations

The significant dispersion of experimental data in both tension and compression calls for a statistical characterization of mechanical properties of the adobe bricks under study. In fact, a conservative way to develop a mechanical model may be based on the assumption of characteristic values for strength, elastic moduli, strains, and energy properties. Tensile behavior may be assumed to be elastic-perfectly brittle, so the authors of this study processed only uniaxial compression data for constitutive modeling.

As compression tests were carried out with displacement control, normal stresses were associated with experimental axial strains corresponding to displacement recordings. The problem was that different axial strains were found at each displacement step of the loading process, as a result of different compressive response of specimens. Therefore, denoting by ε_{max} the maximum experimental axial strain imposed during the tests, the range $[0, \varepsilon_{max}]$ was divided into a large number of bins with amplitude $\Delta\varepsilon \ll \varepsilon_{max}$. A single 'reference axial strain' ε_j was then defined as the central value of each jth bin, so that experimental strains ε_i falling in the jth bin were approximated to the same value ε_j and the corresponding normal stress vector $\Sigma(\varepsilon_j)$ was introduced. The stress vector included a "section" of normal stresses $\sigma_i(\varepsilon_j)$ corresponding to multiple compression tests (where $i = 1, \ldots, 34$) and the reference strain of the jth bin. This procedure allowed the authors to perform a sectional data analysis, namely to derive statistics of the sectional distribution of normal stresses $\sigma_i(\varepsilon_j)$ at each jth strain level ranging in the interval $[0, \varepsilon_{max}]$. In particular, the 5th, 50th and 95th percentiles of normal stresses were estimated through classical statistical procedures.

Sectional data analysis then provided a data set of normal stresses for each percentile under consideration. Thus, regression analysis was carried out for the three stress–strain data sets corresponding to those percentiles, in order to obtain simplified constitutive equations for structural design/assessment purposes. It is noted that regression analysis provides the conditional expectation of the dependent variable y given the independent variable x, namely the mean of the dependent variable under a given value of the independent variable. This calls for the quantification of the coefficient of determination R^2 for each regression model, to measure how well the model fits the experimental data. This means that the empirical constitutive model derived by regression analysis for each percentile of normal stresses provides their expected value under varying axial strain.

Fig. 9 shows the stress–strain data sets and fitted models corresponding to the three percentile levels under consideration. The characteristic and median stress–strain relationships, namely the equations that respectively provide the 5th and 50th percentiles of normal stresses under a given axial strain, are defined as follows (with $R^2 = 0.99$ and $R^2 = 0.98$ respectively):

$$\sigma c=38.24\varepsilon-991.40\varepsilon 2 \quad (6)$$

$$\sigma c=60.14\varepsilon-1458\varepsilon 2 \quad (7)$$

whereas the constitutive equation at the 95th percentile is (R^2 = 0.94):(8)

$$\sigma c=86.70\varepsilon-1152\varepsilon 2 \quad (8)$$

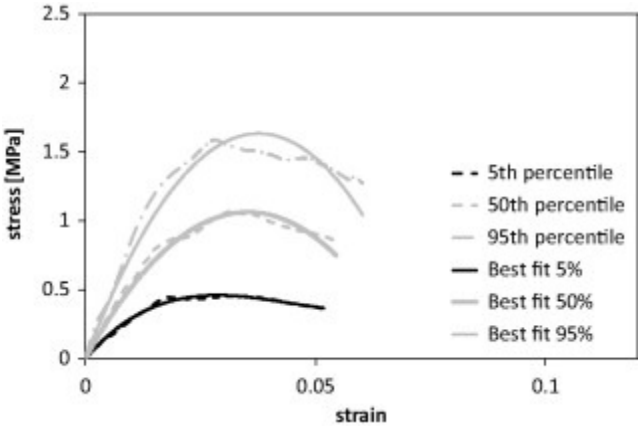

Fig. 9. Strength-degrading nonlinear stress–strain diagrams in compression at different percentile levels.

Such equations are sufficiently simple to be used in engineering practice, allowing one to directly derive the stress–strain behavior at different percentile levels and also to simulate the softening behavior of adobe bricks in compression. It is emphasized that experimental stress–strain curves were truncated at the ultimate strain (that is, 20% strength drop), consistently with the EPP models presented above. In addition, it is noted that the distinction between characteristic and median constitutive models is important for structural applications, because current building codes such as IBC [24] and Eurocode 8 [46] recommend the use of characteristic properties in linear equivalent analysis procedures and median properties in nonlinear analysis procedures. In the case of existing buildings, their structural assessment should be based on the use of characteristic or median properties depending on the knowledge level reached through documentation, inspections and testing [24], [46]. Nevertheless, design constitutive equations where stresses are normalized by the peak compressive strength are often used as they can be adopted for different materials, regardless of the actual strength. After that the stress–strain curves related to the three percentile levels were scaled, a constrained nonlinear regression analysis was carried out to fit an additional quadratic polynomial with peak ordinate equal to unity. Such a procedure allowed the authors to derive the following normalized design equation:

$$\sigma cfc=59.81\varepsilon-894.26\varepsilon 2 \quad (9)$$

with $R2$ = 0.96.

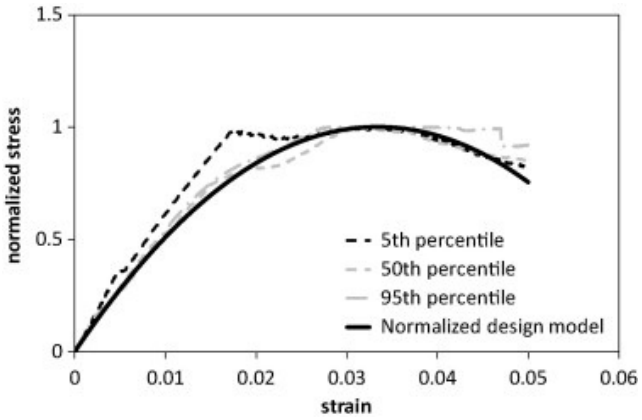

Fig. 10. Normalized design stress–strain diagram for uniaxial compression compared to normalized percentile curves.

5. Conclusions

Straw fiber reinforced adobe bricks used in Sardinia (Italy) and produced according to traditional worldwide handcrafted manufacturing procedures have been experimentally characterized through: (1) particle size distribution analysis of the soil; (2) statistical analysis of straw fiber reinforcement; and (3) compression and three-point bending tests performed in displacement control up to a near failure state. Experimental results can be summarized as follows:

- The length of straw fibers used for the case-study adobe bricks can be assumed to be lognormally distributed in micromechanical modeling. The uncertainty affecting fiber diameter is rather low.
- Based on compression tests, statistics for peak strength, axial strain at peak strength, secant Young's modulus and fracture energy were obtained. A linear correlation between compressive Young's modulus and peak compressive strength has been proposed, while both linear and quadratic correlations between compressive fracture energy and peak compressive strength were derived. Finally, two types of characteristic and mean stress–strain relationships have been proposed for design and assessment purposes: the EPP model and full nonlinear constitutive model with softening. A normalized design equation for uniaxial compression has been also proposed to be used for adobe units with different peak strength.
- Based on three-point bending tests, both peak tensile strength and tensile Young's modulus were estimated. Mean tensile strength has been found to be half of mean compressive strength. Tensile Young's modulus was evaluated through a procedure based on Euler–Bernoulli beam theory and homogenization of mid section, accounting for variability in compressive Young's modulus. That analysis has shown that the adobe material under study can be considered a bimodulus material.

Acknowledgements

This research was carried out in the framework of PON 01-02324 PROVACI project (Technologies for Earthquake Protection and Valorization of Cultural Heritage Sites), CRP-48693 project (dealing

with seismic assessment of adobe structures under low-intensity earthquakes including Sardinia, Italy) and DPC-ReLUIS 2014 project (Line 1 – Masonry Structures), which were respectively funded by the Italian Ministry of Education, University and Research, Regione Sardegna (Regional Law 7/8/2007, n. 7), and Italian Civil Protection Department.

References

[1]G. Minke Building with earth – design and technology of a sustainable architecture Birkhäuser, Basel (2006)
[2] B. Berge The ecology of building materials (2nd ed), Architectural Press, Elsevier Science (2009)
[3]H. Guillaud Characterization of earthen materials
[4]E. Avrami, H. Guillaud, M. Hardy (Eds.), Terra literature review – an overview of research in earthen architecture conservation, The Getty Conservation Institute, Los Angeles (2008), pp. 21-31 World heritage earthen architecture programme (WHEAP). World heritage, inventory and condition of properties built with earth. Draft report, <http://unesdoc.unesco.org/images/0021/002170/217020e.pdf>; 2011 [accessed 22.08.13].
[5] C.H. Kouakou, J.C. Morel Strength and elasto-plastic properties of non-industrial building materials manufactured with clay as a natural binder. Appl Clay Sci, 44 (1–2) (2009), pp. 27-34
[6]Q.-B. Bui, J.C. Morel, S. Hans, N. Meunier Compression behaviour of non-industrial materials in civil engineering by three scale experiments: the case of rammed earth. Mater Struct, 42 (8) (2009), pp. 1101-1116
[7]M.C.J. Delgado, I.C. Guerrero Earth building in Spain. Constr Build Mater, 20 (9) (2006), pp. 679-690
[8]M. Bouhicha, F. Aouissi, S. Kenai Performance of composite soil reinforced with barley straw Cem Concr Compos, 27 (5) (2005), pp. 617-621
[9]H. Binici, O. Aksogan, T. Shah Investigation of fibre reinforced mud brick as a building material Constr Build Mater, 19 (4) (2005), pp. 313-318
[10]F. Fratini, E. Pecchioni, L. Rovero, U. Tonietti The earth in the architecture of the historical centre of Lamezia Terme (Italy): characterization for restoration. Appl Clay Sci, 53 (3) (2011), pp. 509-516
[11]A. Sanna, C. AtzeniArchitettura in terra cruda DEI, Rome (2009). [in Italian]
[12]H. Houben, H. Guillaud Earth construction – a comprehensive guide. Intermediate Technology Publication, London (1994)
[13]A. Caporale, F. Parisi, D. Asprone, R. Luciano, A. Prota Critical surfaces for adobe masonry: micromechanical approach. Compos Part B, 56 (2014), pp. 790-796
[14]A. Caporale, F. Parisi, D. Asprone, R. Luciano, A. Prota Micromechanical analysis of adobe masonry as two-component composite: influence of bond and loading schemes Compos Struct, 112 (2014), pp. 254-263
[15]A. Caporale, F. Parisi, D. Asprone, R. Luciano, A. Prota Comparative micromechanical assessment of adobe and clay brick masonry assemblages based on experimental data sets Compos Struct, 120 (2015), pp. 208-220
[16]ASTM D 2487-11. Standard practice for classification of soils for engineering purposes (unified soil classification system). West Conshohocken: ASTM International; 2011.
[17]M. Achenza, U. Sanna (Eds.), Il manuale tematico della terra cruda, DEI, Rome (2009) [in Italian]
[18]F. Aymerich, L. Fenu, P. Meloni Effect of reinforcing wool fibres on fracture and energy absorption properties of an earthen material Constr Build Mater, 27 (1) (2012), pp. 66-72

[19]EN 1926. Natural stone test methods – determination of compressive strength. Brussels: Comité Européen de Normalisation; 1999.
[20]ASTM E 11–04. Standard tests method for Young's modulus, tangent modulus, and chord modulus. West Conshohocken: ASTM International; 2004.
[21]D. Silveira, H. Varum, A. Costa, T. Martins, H. Pereira, J. Almeida Mechanical properties of adobe bricks in ancient constructionsConstr Build Mater, 28 (1) (2012), pp. 36-44
[22]NZS 4297:1998. Engineering design of earth buildings. Wellington: Standards New Zealand; 1998.
[23]Lourenço PB. Computational strategies for masonry structures [Ph.D. thesis]. Delft University of Technology, Delft, The Netherlands; 1996.
[24]Italian Building Code (IBC). D.M. 14.01.2008: Norme Tecniche per le Costruzioni. Rome: Italian Ministry of Infrastructures and Transportation; 2008 [in Italian].
[25]F. Parisi, N. Augenti Assessment of unreinforced masonry cross sections under eccentric compression accounting for strain softening Constr Build Mater, 41 (2013), pp. 654-664
[26]14.7.4 New Mexico Earthen building materials code. Santa Fe, New Mexico (USA): Construction industries division of the regulation and licensing department; 2009.
[27]ASTM standard E2392/E2392M – 10e1. Standard guide for design of earthen wall building systems. West Conshohocken: ASTM International; 2010.
[28]Compressed earth blocks: materials identification tests and mechanical tests. Lyon: ENTPE/CRATerre-EAG; 1998.
[29]NZS 4298:1998. Materials and workmanship for earth buildings. Wellington: Standards New Zealand; 1998.
[30]EN 1015–11. Methods of test for mortar for masonry – part 11: determination of flexural and compressive strength of hardened mortar. Brussels: Comité Européen de Normalisation; 1999
[30]EN 1015–11. Methods of test for mortar for masonry – part 11: determination of flexural and compressive strength of hardened mortar. Brussels: Comité Européen de Normalisation; 1999.
[31]R.M. Jones Stress–strain relations for materials with different moduli in tension and compression AIAA J, 15 (1977), pp. 16-23
[32]S.A. Ambartsumyan Elasticity theory of different moduli China Railway Publishing House, Beijing (1986)
[33]M. Achenza, L. Fenu On earth stabilization with natural polymers for earth masonry construction. Mater Struct, 39 (1) (2006), pp. 21-27
[34]E. Adorni, E. Coïsson, D. Ferretti In situ characterization of archaeological adobe bricks Constr Build Mater, 40 (2013), pp. 1-9
[35] Baglioni E, Fratini F, Rovero L. The materials utilised in the earthen buildings sited in the Drâa Valley (Morocco): mineralogical and mechanical characteristics. In: Proceedings of 6° Seminário de Arquitectura de Terra em Portugal and 9° Seminário Ibero-Americano de Construção e Arquitectura com Terra [CD-ROM], Coimbra, Portugal; February 20–23; 2010.
[36]A. Figueiredo, H. Varum, A. Costa, D. Silveira, C. Oliveira. Seismic retrofitting solution of an adobe masonry wall. Mater Struct, 46 (1–2) (2013), pp. 203-219
[37]C. Galán-Marín, C. Rivera-Gómez, J. Petric. Clay-based composite stabilized with natural polymer and fibre. Constr Build Mater, 24 (8) (2010), pp. 1462-1468
[38]Gavrilovic P, Sendova V, Ginell WS, Tolles L. Behaviour of adobe structures during shaking table tests and earthquakes. In: Proceedings of the 11th European conference on earthquake engineering [CD-ROM], Rotterdam, Netherlands; September 6–11; 1998.
[39]Lenci S, Piattoni Q, Clementi F, Sadowski T. A mechanical characterization of unfired dry earth: ultimate strength, damage and fracture parameters. In: Proceedings of 19th AIMETA conference Ancona. Paper No. 140; 2009.
[40]D. Liberatore, G. Spera, M. Mucciarelli, M.R. Gallipoli, D. Santarsiero, C. Tancredi. Typological and experimental investigation on the adobe buildings of Aliano (Basilicata, Italy)

P.B. Lourenço, P. Roca, C. Modena, S. Agrawal (Eds.), Proceedings of the 5th international conference on structural analysis of historical constructions, Macmillan India, India (2006), pp. 851-858 November 6–8
[41]Meli R. Experiences in Mexico on the reduction of seismic vulnerability of adobe constructions. In: Proceedings of SismoAdobe2005 [CD-ROM], Lima, Peru; May 16–19; 2005 [in Spanish].
[42]J.C. Rivera, E.E. Muñoz Structural characterization of materials of earth structural systems: adobe. Revista Internacional de Desastres Naturales Accidentes e Infraestructura Civil, 5 (2) (2005), pp. 135-148 [in Spanish]
[43]D. Silveira, H. Varum, A. Costa Influence of the testing procedures in the mechanical characterization of adobe bricks Constr Build Mater, 40 (2013), pp. 719-728
[44]F. Wu, G. Li, H.-N. Li, J.-Q. Ji Strength and stress–strain characteristics of traditional adobe block and masonry Mater Struct, 46 (2013), pp. 1449-1457
[45]
[45]Ş. Yetgin, Ö. Çavdar, A. Çavdar The effects of the fiber contents on the mechanic properties of the adobes Constr Build Mater, 22 (3) (2008), pp. 222-227
[46]EN 1998. Eurocode 8: Design of structures for earthquake resistance. Comité Européen de Normalisation, Brussels; 2004 (Part 1) and 2005 (Part 3).